JOURNAL OF AGRICULTURAL AND FOOD CHEMISTRY

Article

Tailoring natural abenquines to inhibit the photosynthetic electron transport through interaction with the D1 protein in photosystem II

Amalyn Nain-Perez, Luiz C. A. Barbosa, Celia RA Maltha, Samuele Gilberti, and Giuseppe Forlani

J. Agric. Food Chem., **Just Accepted Manuscript** • DOI: 10.1021/acs.jafc.7b04624 • Publication Date (Web): 01 Dec 2017

Tailoring Natural Abenquines to Inhibit the Photosynthetic Electron Transport through Interaction with the D1 Protein in Photosystem II

Amalyn Nain-Perez,[†] Luiz C. A. Barbosa,[*,†,‡] Celia R. A. Maltha,[‡] Samuele Giberti[§] and Giuseppe Forlani[*,§]

[†] Department of Chemistry, Universidade Federal de Minas Gerais, Av. Pres. Antônio Carlos, 6627, Campus Pampulha, CEP 31270-901, Belo Horizonte, MG, Brazil.

[‡] Department of Chemistry, Universidade Federal de Viçosa, Viçosa, Av. P. H. Rolfs s/n, CEP 36570-000, Viçosa, MG, Brazil.

[§] Department of Life Science and Biotechnology, University of Ferrara, via L. Borsari 46, I-44121 Ferrara, Italy.

[*]Corresponding author:
Phone: +55 31 38993068. Fax: +55 31 38993065. E-mail: lcab@ufmg.br.
Phone: +39 0532 455311. Fax: +39 0532 249761. E-mail: flg@unife.it.

ABSTRACT

Abenquines are natural *N*-acetylaminobenzoquinones bearing amino acids residues, which act as weak inhibitors of the photosynthetic electron transport chain. Aiming to exploit the abenquine scaffold as a model for the synthesis of new herbicides targeting photosynthesis, fourteen new analogues were prepared by replacing the amino acid residue with benzylamines and the acetyl with different acyl groups. The synthesis was accomplished in three steps with a 68-95% overall yield from readily available 2,5-dimethoxyaniline, acyl chlorides and benzyl amines. Key steps include (i) acylation of the aniline, (ii) oxidation, and (iii) oxidative addition of the benzylamino moiety. The compounds were assayed for their activity as Hill inhibitors, under basal, uncoupled or phosphorylating conditions, or excluding photosystem I. Four analogues showed high effectiveness (IC_{50} = 0.1-0.4 μM), comparable with the commercial herbicide diuron (IC_{50} = 0.3 μM). The data suggest that this class of compounds interfere at the reducing side of photosystem II, having protein D1 as the most probable target. Molecular docking studies with the plastoquinone binding site of *Spinacia oleracea* further strengthened this proposal.

KEYWORDS

Abenquine analogues; Aminoquinones; Photosynthesis inhibitors; Photosynthetic electron transport; Herbicides

44 **INTRODUCTION**

45 Presently, agricultural pests[1] and weeds[2] are largely controlled by the use of
46 agrochemicals. Since the introduction of the synthetic auxin 2,4-dichlorophenoxyacetic
47 acid (2,4-D) in 1946, herbicides have become the primary tool for weed management.[3,4]
48 Hence, over the years herbicides contributed considerably to increased crop yields,
49 providing a highly effective, economical and relatively simple means for weed control.[3,5]
50 They act through different mechanisms, such as inhibition of amino acids or fatty acids
51 biosynthesis, or interference with microtubule formation, or the photosynthetic electron
52 transport light reactions.[2] However, a continuous use of the same herbicide or herbicides
53 sharing the same target leads to the rapid selection of weed biotypes resistant to such
54 chemicals.[3] The identification and characterization of novel herbicides is therefore highly
55 desirable to manage resistant weeds.[5–7] In the last decade some analogues to natural
56 products have been developed and used as herbicides, but they contribute to only
57 approximately 8% of chemicals used for crop protection.[8] Natural compounds are often
58 environmentally friendly, as their half-life in the soil is usually shorter compared with that
59 of synthetic herbicides.[9,10] Moreover, their wide structural diversity offers opportunities to
60 discover new sites of herbicide action, beyond the targets described to date.[11,12] Several of
61 currently used active principles target the photosynthetic process and these can be
62 classified as 1) electron transport inhibitors, 2) uncouplers, 3) energy transfer inhibitors, 4)
63 inhibitory uncouplers or 5) electron acceptors.[13]

64 During recent years several natural compounds have been investigated for their
65 allelopathic activities.[14–19] Among this large array of natural substances is sorgoleone, a
66 lipophilic quinone produced by *Sorghum bicolor*. The phytotoxic properties of this quinone
67 have been investigated for many years,[20] and its potent herbicidal activity on small-seeded
68 weeds seems due to the interference with the electron transfer process at the photosystem II
69 (PSII) level.[21] On this basis, several sorgoleone analogues were synthesized that showed

herbicidal activity against weeds as *Desmodium tortuosum, Hyptis suaveolens, Hyptis lophanta, Brachiaria decumbens*, and *Euphorbia heterophylla*.[22,23]

Abenquines are natural products isolated from *Streptomyces* sp. strain DB634, a bacterium found in the Atacama Desert in Chile.[24] Abenquines A-D (Figure 1) are *N*-acetylaminobenzoquinones bearing different amino acids residues. We recently described an efficient procedure for their synthesis and of some analogues.[25] Several of them showed a remarkable algicidal activity, inhibiting cyanobacterial growth by 50% at 1.0 μM.[26] However, their mode of action has not been elucidated.

Here we report that abenquine A and some synthetic analogues inhibit the Hill reaction in vitro, and therefore are potentially endowed with phytotoxic and herbicidal activity. Some new synthetic analogues showing increased effectiveness were synthesized. In addition, molecular docking studies were performed aiming to locate their potential site of action in the photosynthetic system. Results indicate that abenquines and some amide analogues interact at the D1 protein level of PSII.

MATERIALS AND METHODS

Synthesis. All reagents were purchased from Sigma-Aldrich and were used without any purification; solvents were procured from Fluka. All compounds were fully characterized by IR, EI-MS, ^{1}H NMR and ^{13}C NMR spectroscopy. Infrared spectra were recorded on a Paragon 1000 FTIR spectrophotometer (Perkin-Elmer, Waltham, MA, USA), preparing the samples as potassium bromide disks (1% w/w). ^{1}H NMR spectra were recorded at 400 MHz and ^{13}C NMR spectra at 100 MHz with an Advance 400 (Bruker, Billerica, MA, U.S.A), using $CDCl_3$ or DMSO-d_6 as solvent and TMS as internal reference. Data are reported as follows: chemical shift (δ), multiplicity (s= singlet, d= doublet, t= triplet, q= quartet, br= broad, m= multiplet), coupling constants (J = Hz) and integration. The mass spectra were recorded on MS-API2000 (Applied Biosystem, Halle, Saale,

96 Germany) under electro spray ionization (ESI). Elemental analyses were measured on a
97 Vario EL unit (Foss-Heraeus, Halle, Saale, Germany). The melting points were measured
98 on an MQAPF-301 apparatus (Microquimica Ldta, Belo Horizonte, MG, Brazil) and are
99 uncorrected. The experimental details for the synthesis of abenquines A-D (**1-4**) and
100 compounds **5-8** and **23** are the same as reported previously.[25]
101
102 **Synthesis of analogues 9-22**
103 **2-Acetamido-5-(2-fluorobenzylamino)-1,4-benzoquinone** (**9**). *Acylation step.* To
104 a round-bottomed flask (50 mL) were added 2,5-dimethoxyaniline (1.0 g, 6.6 mmol) and
105 trimethylamine (1.1 mL, 7.6 mmol) dissolved in dichloromethane (25 mL) at 0 ºC. Then, to
106 the stirred solution was added acetyl chloride (0.6 mL, 7.6 mmol). The resulting solution
107 was warmed to room temperature over 30 min. When TLC analysis revealed the
108 consumption of the starting material, the mixture was washed with water (3 x 25 mL),
109 saturated aqueous sodium hydrogen carbonate solution (25 mL) and brine (25 mL), and
110 then dried over $MgSO_4$. The mixture was filtered and the solvent removed under reduced
111 pressure in a rotary evaporator to give a brown solid. This crude product was used in the
112 next step without further purification.
113 *Oxidation step.* To a round-bottomed flask (50 mL) was added the 2,5-
114 dimethoxyacetanilide previously obtained (1.0 g, 5.1 mmol) in water (25 mL) and MeOH
115 (0.64 mL). The mixture was homogenized by magnetic stirring before a slow addition of
116 phenyl iodine diacetate (2.5 g, 7.7 mmol). The resulting suspension was stirred for 1.5 h,
117 diluted with water (50 mL) and extracted with dichloromethane (3 x 50 mL). The
118 combined extracts were washed with water (50 mL) and saturated aqueous sodium
119 hydrogen carbonate solution (50 mL), dried (Na_2SO_4), filtered and the solvent was
120 concentrated under reduced pressure to afford the required quinone as a brown solid. Since

121 TLC analysis showed only one spot, this crude product was used for the next reaction
122 without purification.

123 *Aza-Michael addition step.* To a round-bottomed flask (25 mL) was added 2-
124 acetamido-1,4-benzoquinone previously obtained (0.12 g, 0.73 mmol) in dichloromethane
125 (5 mL), followed by the addition of 2-fluorobenzylamine (0.10 g, 0.80 mmol). The reaction
126 mixture was stirred at room temperature. Initially, the reaction mixture turned from yellow
127 to red dark. The reaction was quenched after 2 h, before removal of the solvent under
128 reduced pressure to afford the crude product as a dark red residue. This residue was
129 purified by silica gel column chromatography eluting with hexane/EtOAc (7:1 v/v) to
130 afford the required product as red crystals. Overall yield over three steps: 89% (187 mg,
131 0.65 mmol). M.p 231-233 °C. IR (KBr) $\bar{\upsilon}_{max}$ 3290, 2934, 2856, 1725, 1664, 1590, 1500,
132 1470, 1355, 1056, 872 cm^{-1}. ^{1}H NMR (DMSO-d_6, 400 MHz) δ: 9.57 (s, 1H), 8.15 (t, J =
133 6.4 Hz, 1H), 7.30-7.36 (m, 2H), 7.15-7.21 (m, 3H), 5.35 (s, 1H), 4.43 (d, J = 6.4 Hz, 2H),
134 2.18 (s, 3H,). ^{13}C NMR (DMSO-d_6, 100 MHz) δ: 183.4, 178.3, 171.1, 147.9, 141.9, 129.3,
135 124.5, 115.5, 115.1, 109.1, 94.2, 24.5. EIMS *m/z* 286.9 $[M-H]^-$; 311.1 $[M+Na]^+$; analysis
136 for $C_{15}H_{13}FN_2O_3$, C 62.50, H 4.55, N 9.72%; found: C 62.31, H 4.72, N 9.56%.

137

138 The other compounds (**10-22**) were prepared following the same procedure
139 described previously for the synthesis of **9**. The overall yield over three steps are reported.

140

141 **2-Acetamido-5-(4-chlorobenzylamino)-1,4-benzoquinone** (**10**). Red solid. Yield:
142 72% (160 mg, 0.53 mmol). M.p 227-229 °C. IR (KBr) $\bar{\upsilon}_{max}$ 3294, 2924, 2854, 1712, 1654,
143 1588, 1522, 1478, 1342, 1026, 862 cm^{-1}. ^{1}H NMR (DMSO-d_6, 400 MHz) δ: 9.57 (s, 1H),
144 8.30 (s, 1H), 7.39 (d, J = 6.5 Hz, 2H), 7.34 (d, J = 6.5 Hz, 2H), 7.22 (s, 1H), 5.35 (s, 1H),
145 4.39 (brs, 2H), 2.19 (s, 3H). ^{13}C NMR (DMSO-d_6, 100 MHz) δ: 183.6, 178.3, 171.1, 147.9,
146 141.9, 136.2, 131.7, 129.1, 128.4, 109.2, 94.5, 44.3, 24.5. EIMS *m/z* 302.9 $[M-H]^-$; 327.1

147 [M+Na]$^+$; analysis for $C_{15}H_{13}ClN_2O_3$, C 59.12, H 4.30, N 9.19%; found: C 58.92, H 4.41,
148 N 9.02%.

149 **2-Acetamido-5-(3-chlorobenzylamino)-1,4-benzoquinone** (**11**). Red solid. Yield:
150 68% (151 mg, 0.49 mmol). M.p 231-232 °C. IR (KBr) $\bar{\upsilon}_{max}$ 3316, 2336, 2930, 1718, 1660,
151 1582, 1488, 1176, 722 cm^{-1}. ^{1}H NMR (DMSO-$_{d6}$, 400 MHz) δ: 9.57 (s, 1H), 8.30 (s, 1H),
152 7.42 (s, 1H), 7.31-7.38 (m, 3H), 7.23 (s, 1H), 5.39 (s, 1H), 4.41 (d, J = 5.0 Hz, 2H), 2.20
153 (s, 3H). ^{13}C NMR (DMSO-$_{d6}$, 100 MHz) δ: 183.6, 178.4, 171.2, 148.0, 141.9, 139.9, 133.2,
154 130.3, 127.2, 127.1125.9, 109.2, 94.5, 44.4, 24.6. EIMS *m/z* 302.9 [M-H]$^-$; 326.9 [M+Na]$^+$;
155 analysis for $C_{15}H_{13}ClN_2O_3$, C 59.12, H 4.30, N 9.19%; found: C 58.85, H 4.55, N 8.97%.

156 **2-Acetamido-5-(4-nitrobenzylamino)-1,4-benzoquinone** (**12**). Red solid. Yield:
157 76% (175 mg, 0.55 mmol). M.p 250-252 °C. IR (KBr) $\bar{\upsilon}_{max}$ 3292, 2956, 2924, 2856, 1714,
158 1654, 1474, 1260, 1026, 804 cm^{-1}. ^{1}H NMR (DMSO-$_{d6}$, 400 MHz) δ: 9.61 (s, 1H), 8.65 (s,
159 1H), 7.23 (d, J = 6.0 Hz, 2H), 7.61 (d, J = 6.0 Hz, 2H), 7.26 (s, 1H), 5.37 (s, 1H), 4.57 (brs,
160 2H), 2.21 (s, 3H). ^{13}C NMR (DMSO-$_{d6}$, 100 MHz) δ: 183.5, 178.5, 171.2, 148.0, 146.7,
161 145.3, 141.9, 128.3, 123.6, 109.3, 94.7, 44.5, 24.5. EIMS *m/z* 314.4 [M-H]$^-$; 338.4
162 [M+Na]$^+$; analysis for $C_{15}H_{13}N_3O_5$, C 57.14, H 4.16, N 13.33%; found: C 59.94, H 4.30, N
163 13.12%.

164 **2-Acetamido-5-(2-bromobenzylamino)-1,4-benzoquinone** (**13**). Red solid. Yield:
165 85% (217 mg, 0.62 mmol). M.p 225-227 °C. IR (KBr) $\bar{\upsilon}_{max}$ 3280, 2924, 2854, 1708, 1654,
166 1606, 1566, 1490, 1312, 1174, 1024, 750 cm^{-1}. ^{1}H NMR (DMSO-$_{d6}$, 400 MHz) δ: 9.55 (s,
167 1H), 7.61-7.66 (m, 1H), 7.33-7.39 (m, 2H), 7.21-7.26 (m, 1H), 7.13 (s, 1H), 5.58 (s, 1H),
168 4.82 (brs, 2H), 2.18 (s, 3H). ^{13}C NMR (DMSO-$_{d6}$, 100 MHz) δ: 185.1, 178.6, 171.1, 151.1,
169 140.1, 132.7, 132.3, 129.1, 128.0, 127.8, 121.9, 111.6, 100.5, 57.7, 24.5. EIMS *m/z* 346.8
170 [M-H]$^-$; 3.71.0 [M+Na]$^+$; analysis for $C_{15}H_{13}BrN_2O_3$, C 51.59, H 3.75, N 8.02%; found: C
171 51.42, H 3.84, N 7.75%.

2-Acetamido-5-(3-bromobenzylamino)-1,4-benzoquinone (**14**). Red solid. Yield: 92% (235 mg, 0.67 mmol). M.p 213-215 °C. IR (KBr) $\bar{\upsilon}_{max}$ 3316, 3242, 2942, 1716, 1658, 1580, 1488, 1374, 1332, 1176, 718 cm^{-1}. ^{1}H NMR (DMSO-$_{d6}$, 400 MHz) δ: 9.57 (s, 1H), 8.30 (s, 1H), 7.56 (s, 1H), 7.44-7.48 (m, 1H), 7.28-7.36 (m, 2H), 7.24 (s, 1H), 5.39 (s, 1H), 4.41 (d, J = 6.0 Hz, 2H), 2.21 (s, 3H). ^{13}C NMR (DMSO-$_{d6}$, 100 MHz) δ: 183.6, 178.4, 171.1, 147.9, 141.9, 140.1, 130.6, 130.1, 129.9, 126.3, 121.8, 109.2, 94.5, 44.4, 24.5. EIMS *m/z* 347.1 $[M-H]^-$; 371.0 $[M+Na]^+$; analysis for $C_{15}H_{13}BrN_2O_3$, C 62.50, H 4.55, N 9.72%; found: C 62.37, H 4.61, N 9.51%.

2-Acetamido-5-(4-bromobenzylamino)-1,4-benzoquinone (**15**). Red solid. Yield: 78% (199 mg, 0.57 mmol). M.p 222-225 °C.IR (KBr) $\bar{\upsilon}_{max}$ 3294, 2958, 2924, 2854, 1712, 1654, 1588, 1522, 1342, 1176, 1100, 862 cm^{-1}. ^{1}H NMR (DMSO-$_{d6}$, 400 MHz) δ: 9.57 (s, 1H), 8.29 (s, 1H), 7.52 (d, J = 7.7 Hz, 2H), 7.28 (d, J = 7.7 Hz, 2H), 7.21 (s, 1H), 5.33 (s, 1H), 4.36 (d, J = 5.6 Hz, 2H), 2.18 (s, 3H). ^{13}C NMR (DMSO-$_{d6}$, 100 MHz) δ: 183.6, 178.3, 171.1, 147.9, 141.9, 136.7, 131.1, 129.4, 120.2, 109.2, 94.5, 44.4, 24.5. EIMS *m/z* 347.0 $[M-H]^-$; 371.3 $[M+Na]^+$; analysis for $C_{15}H_{13}BrN_2O_3$, C 51.59, H 3.75, N 8.02%; found: C 51.41, H 3.93, N 7.94%.

2-Acetamido-5-(2-methylbenzylamino)-1,4-benzoquinone (**16**). Red solid. Yield: 70% (145 mg, 0.51 mmol). M.p 232-235 °C. IR (KBr) $\bar{\upsilon}_{max}$ 3288, 2922, 2854, 1710, 1654, 1574, 1482, 1348, 1176, 758 cm^{-1}. ^{1}H NMR (DMSO-$_{d6}$, 400 MHz) δ: 9.57 (s, 1H), 8.10 (s, 1H), 7.23 (s, 1H), 7.09-7-18 (m, 4H), 5.27 (s, 1H), 4.36 (d, J = 5.7 Hz, 2H), 2.28 (s, 3H), 2.19 (s, 3H). ^{13}C NMR (DMSO-$_{d6}$, 100 MHz) δ: 183.6, 178.2, 171.2, 148.3, 142.1, 135.6, 134.4, 130.2126.4, 125.8, 109.2, 94.4, 43.5, 24.6, 18.7. EIMS *m/z* 307.1 $[M+Na]^+$; analysis for $C_{16}H_{16}N_2O_3$, C 67.59, H 5.67, N 9.85%; found: C 67.30, H 5.84, N 9.61%.

2-Acetamido-5-(3-methylbenzylamino)-1,4-benzoquinone (**17**). Red solid. Yield: 68% (141 mg, 0.49 mmol). M.p 215-217 °C. IR (KBr) $\bar{\upsilon}_{max}$ 3300, 3286, 3022, 2926, 2858, 1712, 1654, 1572, 1482, 1344, 1176, 768 cm^{-1}. ^{1}H NMR (DMSO-$_{d6}$, 400 MHz) δ: 9.55 (s,

198 1H), 8.24 (s, 1H), 7.19-7.22 (m, 2H, H-3), 7.05-7.11 (m, 3H), 5.32 (s, 1H), 4.34 (d, J = 5.6
199 Hz, 2H), 2.28 (s, 3H), 2.18 (s, 3H). ^{13}C NMR (DMSO-d_6, 100 MHz) δ: 183.7, 178.2, 171.1,
200 148.1, 142.0, 137.6, 137.1, 128.4, 127.8, 127.1, 109.1, 94.4, 45.1, 24.5, 20.9. EIMS *m/z*
201 282.9 [M-H]$^-$; 307.0 [M+Na]$^+$; analysis for $C_{16}H_{16}N_2O_3$, C 62.67.59, H 5.67, N 9.85%;
202 found: C 67.42, H 5.81, N 9.57%.

203 **2-Pentanamido-5-(benzylamino)-1,4-benzoquinone** (**18**). Red crystals. Yield:
204 90% (204 mg, 0.5065mmol). M.p 209-211 °C. IR (KBr) $\bar{\upsilon}_{max}$ 3314, 2970, 2870, 1696,
205 1654, 1600, 1508, 1328, 1178, 870 cm^{-1}. ^{1}H NMR (DMSO-d_6, 400 MHz) δ: 9.44 (s, 1H),
206 8.28 (s, 1H), 7.22-7.31 (m, 6H, H-3), 5.33 (s, 1H), 4.39 (s, 2H), 2.41-2.59 (m, 2H), 1.44-1-
207 53 (m, 2H), 1.19-1.31 (m, 2H), 0.85 (t, J = 7.0 Hz, 3H). ^{13}C NMR (DMSO-d_6, 100 MHz)
208 δ: 183.6, 178.2, 173.9, 148.1, 141.9, 137.1, 128.5, 127.2, 109.0, 94.4, 45.1, 36.2, 26.7,
209 21.6, 13.6. EIMS *m/z* 311.5 [M-H]$^-$; 335.3 [M+Na]$^+$; analysis for $C_{18}H_{20}N_2O_3$, C 69.00, H
210 6.60, N 9.85%; found: C 69.21, H 6.45, N 9.97%.

211 **3-Methylbutamido-5-(benzylamino)-1,4-benzoquinone** (**19**). Red solid. Yield:
212 82% (186 mg, 0.59 mmol). M.p 198-200 °C. IR (KBr) $\bar{\upsilon}_{max}$ 3318, 2975, 2872, 1698, 1652,
213 1605, 1502, 1324, 1179, 880 cm^{-1}. ^{1}H NMR ($CDCl_3$, 400 MHz) δ: 8.53 (brs, 1H), 7.39 (s,
214 1H), 7.25-7.37 (m, 5H), 6.44 (s, br, 1H), 5.47 (s, 1H), 4.33 (d, J = 5.8 Hz, 2H), 2.29 (d, J =
215 7.0 Hz, 2H), 2.12-2.22 (m, 1H), 0.99 (d, J = 6.6 Hz, 6H). ^{13}C NMR ($CDCl_3$, 100 MHz) δ:
216 183.4, 179.3, 172.1, 148.0, 141.2, 135.4, 129.2, 128.4, 127.7, 109.7, 94.9, 47.2, 46.9, 26.1,
217 22.5. EIMS *m/z* 311.3 [M-H]$^-$; 335.7 [M+Na]$^+$; analysis for $C_{18}H_{20}N_2O_3$, C 69.08, H 6.70,
218 N 9.80%; found: C 69.00, H 6.45, N 9.36%.

219 **2-Pivalamido-5-(benzylamino)-1,4-benzoquinone** (**20**). Red solid. Yield: 95%
220 (216 mg, 0.69 mmol). M.p 206-208 °C. IR (KBr) $\bar{\upsilon}_{max}$ 3324, 3090, 3066, 3030, 2970,
221 2932, 2870, 1696, 1654, 1600, 1456, 1256, 992 cm^{-1}. ^{1}H NMR (DMSO-d_6, 400 MHz) δ:
222 8.93 (brs, 1H), 8.44 (brs, 1H), 7.25-7.31 (m, 5H), 7.13 (s, 1H), 5.39 (s, 1H), 4.42 (s, 2H),
223 1.20 (s, 12H). ^{13}C NMR (DMSO-d_6, 100 MHz) δ: 183.2, 177.6, 177.4, 148.6, 141.1, 136.9,

224 128.4, 127.1, 108.4, 93.9, 45.1, 40.2, 26.6. EIMS *m/z* 311.4 $[M-H]^-$; 335.1 $[M+Na]^+$;
225 analysis for $C_{18}H_{20}N_2O_3$, C 69.13, H 6.62, N 9.73%; found: C 69.21, H 6.45, N 9.97%.

226 **2-Isobutyramido-5-(benzylamino)-1,4-benzoquinone** (**21**). Red solid. Yield: 75%
227 (163 mg, 0.54 mmol). M.p 225-228 °C. IR (KBr) $\bar{\upsilon}_{max}$ 3298, 3256, 2972, 2932, 1706,
228 1654, 1592, 1494, 1330, 1178, 734 cm^{-1}. ^1H NMR (DMSO-d_6, 400 MHz) δ: 9.42 (brs, 1H),
229 8.32 (brs, 1H), 7.23-7.33 (m, 6H), 5.36 (s, 1H), 4.40 (s, 2H), 2.97 (brs, 1H), 1.06 (brs, 6H).
230 ^{13}C NMR (DMSO-d_6, 100 MHz) δ: 178.1, 177.8, 155.3, 148.2, 142.1, 137.1, 128.5, 127.2,
231 109.2, 94.4, 45.1, 34.9, 19.1. EIMS *m/z* 297.0 $[M-H]^-$; 299.4 $[M+Na]^+$; analysis for
232 $C_{17}H_{18}N_2O_3$, C 68.21, H 6.23, N 9.27%; found: C 68.44, H 6.08, N 9.39%.

233 **2-((Methoxycarbonyl)amino)-5-(benzylamino)-1,4-benzoquinone** (**22**). Red
234 solid. Yield: 86% (179 mg, 0.62 mmol). M.p 210-212 °C. IR (KBr) $\bar{\upsilon}_{max}$ 3318, 3230, 2946,
235 1742, 1654, 1578, 1370, 1342, 1186, 1050, 866 746 cm^{-1}. ^1H NMR (DMSO-d_6, 400 MHz)
236 δ: 8.69 (s, 1H), 8.35 (s, 1H), 7.25-7.31 (m, 5H), 6.83 (s, 1H), 5.34 (s, 1H), 4.39 (s, 2H),
237 3.70 (s, 3H). ^{13}C NMR (DMSO-d_6, 100 MHz) δ: 182.7, 177.2, 152.8, 148.4, 142.7, 137.1,
238 128.5, 127.2, 107.4, 94.2, 52.9, 45.2. EIMS *m/z* 284.9 $[M-H]^-$; 287.1 $[M-H]^+$; 309.3
239 $[M+Na]^+$; analysis for $C_{15}H_{13}BrN_2O_3$, C 62.77, H 5.11, N 9.57%; found: C 62.93, H 4.93,
240 N 9.79%.

241

242 **Biological Tests**

243 **Measurement of the Photosynthetic Electron Transport.** Photosynthetically
244 active thylakoid membranes were isolated from market spinach (*Spinacia oleracea* L.)
245 leaves. Briefly, 20 g of deveined plant material were resuspended in 100 mL of ice-cold 20
246 mM Tricine/NaOH buffer (pH 8.0) containing 10 mM NaCl, 5 mM $MgCl_2$ and 0.4 M
247 sucrose, and homogenized for 30 s in a blender at maximal speed. The homogenate was
248 filtered through surgical gauze, and the filtrate was centrifuged at 4 °C for 1 min at 500 g;
249 the supernatant was further centrifuged for 10 min at 1500 g. Pelleted chloroplasts were

250 osmotically disrupted by resuspension in sucrose-lacking buffer, immediately diluted 1:1
251 with sucrose-containing buffer, and kept on ice in the dark until used. Following dilution
252 with 80% (v/v) acetone, the chlorophyll content was calculated using the Arnon's formula.
253 The basal rate of photosynthetic electron transport was measured following the light-driven
254 reduction of ferricyanide. Aliquots of membrane preparations corresponding to 15 μg of
255 chlorophyll were incubated at 24 °C in 1 mL cuvettes containing 20 mM tricine/NaOH
256 buffer (pH 8.0), 10 mM NaCl, 5 mM $MgCl_2$, 0.2 M sucrose and 1 mM $K_3[Fe(CN)_6]$. The
257 assay was initiated by exposure to saturating light (800 μmol/m^2/s), and the rate of
258 ferricyanide reduction was measured at 1 min intervals for 20 min in a Novaspec Plus
259 spectrophotometer (GE Healthcare, Milan, Italy) at 420 nm against an exact blank.
260 Activity was calculated over the linear portion of the curve from a molar extinction
261 coefficient of 1000/M/cm. Compounds **6-10** and **17-20** were dissolved in DMSO and then
262 diluted with water, as required. Their effect on the photosynthetic electron transport chain
263 was measured by adding concentrations in the range from 0.1 to 100 μM to the above
264 reaction mixture, and comparing the results with untreated parallel controls. Each assay
265 was repeated in triplicate, and results were expressed as percentage of untreated controls.
266 Phosphorylating photosynthetic electron rate was determined under the same conditions,
267 but in the presence of 0.5 mM ADP and 2 mM K_2HPO_4. Uncoupled photosynthetic
268 electron rate was measured following the addition of 1 mM NH_4Cl to the basal reaction
269 mixture. In these last two cases, ferricyanide reduction was determined at intervals of 30 s
270 for 10 min. Reported values are mean ± SE over replicates. The concentrations causing
271 50% inhibition (IC_{50}) and their confidence limits were estimated by nonlinear regression
272 analysis using Prism 6 for Windows, version 6.03 (GraphPad Software, La Jolla, CA).

273 **Molecular docking.** Molecular docking studies for compounds **5**, **10**, **14**, **15**, **21**
274 and lenacil with the active site of spinach photosystem II (PDB: 3JCU) were performed by
275 using AutoDockTools 4.2 program suite.[27,28] Each compound was generated using

276 ChemDraw 14.0 followed by MM2 energy minimization. The target enzyme was prepared
277 for molecular docking simulation using the chain A by removing water, and all hydrogens
278 were added, Gasteiger charges were calculated and non-polar hydrogens were merged to
279 carbon atoms. A grid box size of 40 x 40 x 40 point (x, y, z) with a spacing of 0.486 Å was
280 centered on the X, Y, and Z at -41.788, 3.115, and -18.728, respectively. Then, to evaluate
281 the binding free energy of the inhibitor–macromolecule, automated docking studies were
282 carried out. The genetic algorithm with local search (GALS) was used to find the best
283 conformers. The Lamarckian genetic algorithm with default settings was used as well.
284 Each docking experiment was performed 50 times, yielding 50 docked conformations.
285
286 **RESULTS AND DISCUSSION**
287
288 **Abenquine A is a mild inhibitor of the photosynthetic electron transport, but**
289 **some of its synthetic analogues show a remarkable activity.** Natural abenquines and
290 some synthetic analogues were recently found to inhibit the photoautotrophic growth of a
291 model cyanobacterial strain.[25,26] In photosynthetic organisms, plastoquinone plays a central
292 role carrying electrons from PSII to the cytochrome b_6f complex.[29] Therefore, we
293 investigated the ability of abenquines to interfere with the chloroplast electron transport
294 chain by measuring the Hill reaction using thylakoid membranes isolated from spinach
295 leaves.[30,31] For this initial investigation, natural abenquines A-D and their synthetic
296 analogues **5-8** were prepared in high yields using the methodology previously developed.[25]
297 The results from such bioassays (Table 1) showed that they may indeed exert a significant
298 inhibition of ferricyanide reduction. Natural abenquines were inactive or scarcely active.
299 Only abenquine A reduced electron transport rate at submillimolar concentrations.
300 Remarkably, however, some synthetic analogues were much more effective, with IC_{50}

301 values lower than 100 μM. Moreover one of them, namely compound **5** (IC_{50}= 1.1 μM),
302 was almost as active as diuron,[32] a commercial herbicide targeting PSII (IC_{50} 0.3 μM).
303
304 **Tailoring the abenquine scaffold by replacing the amino acid residue for**
305 **substituted benzylamine groups, or changing the acetyl group by other acyl groups,**
306 **afforded new analogues with increased effectiveness.** Aiming to obtain more active
307 molecules that could be potentially developed as new active principles for weed control,
308 new abenquine analogues were prepared by employing a synthetic methodology that
309 involves a three-step protocol.[25] An initial acylation of 2,5-dimethoxyaniline with the
310 corresponding acyl chloride afforded the required amides in quantitative yields. These
311 amides were immediately oxidized with phenyl iodine diacetate affording the
312 corresponding quinones. Final treatment of crude quinones with a diversity of amines
313 resulted in the isolation of required products (**9-22**) in overall yields ranging from 68 to
314 95% (Figure 2). Based on the fact that analogue **5** bearing an acetyl and a *N*-benzyl moiety
315 was the most active, one set of compounds was prepared keeping the acetyl unit and
316 modifying the substituents on the *N*-benzyl group in order to evaluate the stereo-electronic
317 effect on this portion of the molecule. For another set of compounds, the *N*-benzyl group
318 was kept unchanged and the acyl portion was modified in order to evaluate its size effect.
319 Standard spectroscopic analysis was carried out for structural characterization of
320 these new compounds. In short, mass spectra obtained under electrospray conditions (EI-
321 MS) showed the characteristic molecular ions as expected for each compound. The IR
322 spectra showed absorption bands characteristics of NH, C=O and C=C bonds.[33] On the
323 other hand, the ^{1}H NMR spectra showed a similar pattern for all compounds, with signals
324 at δ 2.18-2.22 corresponding to the methyl group ($\underline{CH_3}$-CO), as well the methylene of
325 benzylamine fragment (-$\underline{CH_2}$-NH) as doublet at δ 4.36-4.81. The aromatic portion of the
326 molecules showed signals in the range of δ 7.04-8.23. The signals corresponding to the N-

327 H amine were observed at δ 8.09-8.40 due to the N-H amide were at δ 9.55-9.60. In the ^{13}C
328 NMR spectra were observed signals corresponded to the methyl group ($\underline{CH_3}$-CO) at δ 24.5-
329 24.6 as well the methylene of benzylamine fragment (-$\underline{CH_2}$-NH) at δ 43.5-57.7. The signals
330 due to carbons of the amide carbonyl groups appeared around 171 ppm.

331 All analogues (**9-22**) were tested for their ability to interfere with the light-driven
332 reduction of ferricyanide by spinach chloroplasts, and the results are summarized in Table
333 2. Among compounds **9-17**, which share the acetamide moiety attached to the quinone
334 core, compounds **9** (*o*-fluoro-substitution) and **12** (*p*-nitro-substitution) bearing a strong
335 electron withdrawing group showed IC_{50} values in the 10 to 100 μM range, whereas
336 compounds with Cl or Br atom in either *meta* or *para*-position (**10** and **11**; **14** and **15**)
337 exhibited IC_{50} values as low as 0.18-0.37 μM, comparable to that found for the herbicide
338 diuron (IC_{50} 0.3 μM).[32] Compound **13**, with Br atom in *ortho*-position, was significantly
339 less effective (IC_{50} = 4.7 μM). A similarity tendency was observed also with a methyl
340 substituent, which in the *ortho*-position (**16**) resulted in an IC_{50} value of 3.6 μM, whereas
341 in the *meta*-position (**17**) exhibited an IC_{50} value of 0.38 μM. Even though no clear
342 structure-activity relationship can be deduced at this stage due to the limited number of
343 analogues evaluated, we observed that the analogues bearing substituent in *meta*-position
344 are better inhibitors of the photosynthetic electron transport. From such preliminary data it
345 is clear that the electronic nature and position of the substituent on the benzyl ring is
346 associated with the activity.

347 The second set of compounds has a benzylamine moiety in the quinone core but
348 bear a different aliphatic chain on the amide group (**18-22**). For comparison purpose
349 compound **23** is included in Table 2. This compound bears a benzoyl group in place of the
350 acetyl group. From the data presented (Table 2), compound **20** with the *tert*-butyl moiety
351 was inactive, and **19** with isobutyl group was scarcely effective. Compound **23** having the

352 large benzene ring was also virtually inactive, causing only 24% inhibition at 100 μM.
353 However, compound **18** with *n*-butyl exerted a moderate inhibition (IC_{50} = 2.6 μM). On the
354 other hand, compounds **21** (bearing an isopropyl group) and **22** (a carbamate) showed IC_{50}
355 values as low as 0.27 and 0.95 μM, respectively. If compared with the IC_{50} value for **5** (1.1
356 μM), this result clearly suggests that the acyl group volume influences the inhibitory
357 potential, with the activity reducing as the steric hindrance increases. However, it seems
358 that the best size for the acyl group is isopropyl, since derivative **21** is approximately 4
359 times more effective than **5**. Also, the only carbamate derivative **22** was as active as **5**,
360 indicating that the target site can also accommodate this pharmacophore. Considering that
361 the previously reported 2,5-bis(alkylamino)-1,4-benzoquinones did not inhibit the Hill
362 reaction at 100 μM and caused only 10% inhibition at 200 μM, being less active than its
363 benzoyl analogue **23** (Table 2),[31] we suggest that the carbonyl group attached to one of the
364 nitrogen atoms is essential for activity, most likely for some hydrogen bond formation in
365 the active site, while a group attached to it should also have an optimal size to fit into the
366 cavity of the reactive center.
367
368 **Both the evaluation of the inhibitory effect of abenquine analogues on the**
369 **photosynthetic electron transport chain under different conditions and docking**
370 **studies suggest the PSII protein D1 as their likely target.** The activity of the most potent
371 abenquine analogues (**10**, **14**, **15**, **21**) was further characterized. The comparison of the
372 inhibitory patterns under basal, uncoupling or phosphorylating conditions (Figure 3)
373 allowed us to rule out the possibility that these compounds may act as energy coupling
374 inhibitors or as uncouplers, thereby impeding ATP synthesis.[34]
375 Being true Hill inhibitors, other experiments were performed to identify their
376 molecular target inside the so called Z scheme, *i.e.* if they interact with the photosynthetic
377 machinery at the photosystem II, cytochrome b_6f complex or photosystem I level.[4,29] When

378 the electron flow was suppressed by addition of the cytochrome b_6f inhibitor 2,5-dibromo-
379 3-methyl-6-isopropyl-*p*-benzoquinone (2 μM), and then an electron flow excluding
380 photosystem I was established by the addition of 0.1 mM phenylenediamine, compounds
381 **10**, **14**, **15**, **21** were still inhibitory (Figure 4). Consequently, the compounds studied here
382 are most likely interacting with the PSII.

383 The great majority of herbicides inhibiting PSII are known to displace the
384 plastoquinone Q_B from its binding site and to inhibit the electron transfer from Q_A to
385 Q_B.[35,36] *In silico* analyses of the interaction between some of these herbicides, such as
386 diuron (3-(3,4-dichlorophenyl)-1,1-dimethylurea), atrazine, terbutryn and bromacil, and the
387 plastoquinone binding site have been carried out using the structure of PSII from either
388 bacteria, like *Rhodopseudomonas viridis*,[37] *Tricondyloides elongatus*,[36,38] *T. vulcanus*,[39]
389 and *Blastochloris viridis*,[40] or plants, like *Phalaris minor*[41] and *Spinacia oleracea*.[39] For
390 the natural quinone sorgoleone a docking study using the Q_B-binding site of the PSII
391 complex of bacterium *Rhodopseudomonas viridis* was carried out.[42] In the current work a
392 docking analysis was performed for the most active abenquine analogues (**5**, **10**, **14**, **15**,
393 **21)** and the herbicide lenacil using the program AutoDockTools 4.2.[27,28] Molecular
394 docking was carried out by using the crystallographic structure of the reaction center of
395 PSII (D1) from spinach (PDB ID: 3JCU). Results suggested that compounds **14** and **15** are
396 bonded *via* oxygen and hydrogen. The carbonyl group of the quinone interacts with an OH
397 of Ser_{264} in 2.063 Å for **14**, or with both Ser_{264} and the NH of the His_{215} with a distance
398 bond of 2.094 and 2.226 Å, for **15** (Figure 5), with docking scores of -7.83 for **14** and -7.69
399 for **15**. Moreover, hydrophobic interactions were found with Phe_{265}, Phe_{274}, Phe_{255}, His_{252},
400 Leu_{271}, Leu_{218} and His_{215} for **14**, and Phe_{255}, Phe_{274}, His_{252}, Leu_{271}, Ala_{251}, Leu_{218} and
401 Met_{214} for **15**. Consequently, the compounds **14** and **15** are surrounded by the above
402 residues. Thus, the interaction of the ligands with these residues might lead to an inhibition
403 of PSII (D1). In addition, most of the herbicides described above prefer the position near

404 the loop made by Ser_{264}, and Phe_{265} in the PSII. The same orientation for abequine
405 analogues **5**, **10**, **14**, **15**, **21** and lenacil herbicide in the binding site was observed.
406
407 In summary, based on the initial observation that natural abenquine A inhibits the
408 electron transport chain in the 10^{-4}-10^{-3} M range, we carried out the synthesis of new, more
409 active analogues. The remarkable biological activity of analogue **5** bearing a benzyl group
410 indicated that such a group is critical for the inhibition of the photosynthetic machinery. In
411 addition, new analogues bearing several substituents in the benzylic ring (**9-17**) or in the
412 amide moiety (**18-22**) were synthesized, with Cl, Br or methyl aromatic substituents
413 resulting in potent inhibitors of the Hill reaction, with IC_{50} values (0.1-0.4 μM) of the same
414 order of magnitude as some commercial herbicides targeting PSII.
415
416 **ASSOCIATED CONTENT**
417 **Supporting Information**
418 Figure of molecular docking and ^{1}H and ^{13}C NMR spectra for synthetic abenquines
419 analogues. This material is available free of charge via the Internet at http://pubs.acs.org
420
421 **AUTHOR INFORMATION**
422 **Corresponding authors**
423 *(L.C.A.B.) Phone: +55 31 38993068. Fax: +55 31 38993065. E-mail: lcab@ufmg.br.
424 *(G.F.) Phone: +39 0532 455311. Fax: +39 0532 249761. E-mail: flg@unife.it.
425 **ORCID**
426 Luiz Cláudio Almeida Barbosa: 0000-0002-5395-9608
427 Giuseppe Forlani: 0000-0003-2598-5718
428 **Notes**
429 The authors declare no competing financial interest.

ACKNOWLEDGEMENTS

We are grateful to the following Brazilian agencies: Conselho Nacional de Desenvolvimento Cientifíco e Tecnológico (CNPq, grant 400746-2014) for research fellowships (L.C.A.B.); Fundação de Amparo à Pesquisa de Minas Gerais (FAPEMIG, grant APQ1557-15) for financial support; and Coordenação de Aperfeiçoamento de Pessoal de Nível Superior (CAPES) for a research fellowship (A.N.P). Support from the University of Ferrara (Fondo di Ateneo per la Ricerca 2016) is also acknowledged. The authors thank Dr R. Csuk for mass spectra data and elemental analysis experiments, and Dr A. Straforini for technical assistance.

REFERENCE

(1) Duke, S. O.; Cantrell, C. L.; Meepagala, K. M.; Wedge, D. E.; Tabanca, N.; Schrader, K. K. Natural toxins for use in pest management. *Toxins (Basel).* **2010**, *2*, 1943–1962.

(2) Baucom, R. S. The remarkable repeated evolution of herbicide resistance. *Am. J. Bot.* **2016**, *103*, 1–3.

(3) Shaner, D. L. Lessons learned from the history of herbicide resistance. *Weed Sci.* **2014**, *62*, 427–431.

(4) Teixeira, R. R.; Pereira, J. L.; Pereira, W. L. Photosynthetic inhibitors. In *Applied Photosynthesis*; Najafpour, M. M., Ed.; InTech, **2012**; pp 3–22.

(5) Heap, I. Global perspective of herbicide-resistant weeds. *Pest Manag. Sci.* **2014**, *70*, 1306–1315.

(6) Burgos, N. R.; Tranel, P. J.; Streibig, J. C.; Davis, V. M.; Shaner, D.; Norsworthy, J. K.; Ritz, C. Review: Confirmation of resistance to herbicides and evaluation of resistance levels. *Weed Sci.* **2012**, *61*, 4–20.

(7) Powles, S. B.; Yu, Q. Evolution in action: plants resistant to herbicides. *Annu. Rev.*

459 *Plant Biol.* **2010**, *61*, 317–347.
460 (8) Cantrell, C. L.; Dayan, F. E.; Duke, S. O. Natural products as sources for new
461 pesticides. *J. Nat. Prod.* **2012**, *75*, 1231–1242.
462 (9) Duke, S. O.; Dayan, F. E.; Romagni, J. G.; Rimando, A. M. Natural products as
463 sources of herbicides: current status and future trends. *Weed Res.* **2000**, *40*, 99–111.
464 (10) Soltys, D.; Krasuska, U.; Bogatek, R.; Gniazdowska, A. Allelochemicals as
465 bioherbicides – pesent and perspectives. *Herbic. - Curr. Res. Case Stud. Use* **2013**,
466 517–542.
467 (11) Jablonkai, I. Molecular mechanism of action of herbicides. In *Herbicides –*
468 *Mechanisms and Mode of Action*; **2011**, pp 3–24.
469 (12) Dayan, F. E.; Duke, S. O. Natural compounds as next generation herbicides. *Plant*
470 *Physiol.* **2014**, *166*, 1090–1105.
471 (13) Fuerst, P. E.; Norman, M. A. Interactions of herbicides with photosynthetic electron
472 transport. *Weed Sci.* **1991**, *39*, 458–464.
473 (14) Macias, F. A.; Galino, J. C. G.; Molinillo, J. M. G. Allelopathy: chemistry and mode
474 of action of allelochemicals; CRC Press. Taylor & Francis Group, **2003**.
475 (15) Barbosa, L. C. A.; Demuner, A. J.; de Alvarenga, E. S.; Oliveira, A.; King-Diaz, B.;
476 Lotina-Hennsen, B. Phytogrowth- and photosynthesis-inhibiting properties of
477 nostoclide analogues. *Pest Manag. Sci.* **2006**, *62,* 214–222.
478 (16) Morales-Flores, F.; Aguilar, M. I.; King-Díaz, B.; Lotina-Hennsen, B. Derivatives
479 of diterpen labdane-8α,15-diol as photosynthetic inhibitors in spinach chloroplasts
480 and growth plant inhibitors. *J. Photochem. Photobiol. B Biol.* **2013**, *125*, 42–50.
481 (17) Macías, F. A.; Marín, D.; Oliveros-Bastidas, A.; Molinillo, J. M. G. Optimization of
482 benzoxazinones as natural herbicide models by lipophilicity enhancement. *J. Agric.*
483 *Food Chem.* **2006**, *54*, 9357–9365.
484 (18) Macías-Rubalcava, M. L.; Ruiz-Velasco Sobrino, M. E.; Meléndez-González, C.;
485 King-Díaz, B.; Lotina-Hennsen, B. Selected phytotoxins and organic extracts from
486 endophytic fungus *Edenia gomezpompae* as light reaction of photosynthesis
487 inhibitors. *J. Photochem. Photobiol. B Biol.* **2014**, *138*, 17–26.
488 (19) King-Díaz, B.; Granados-Pineda, J.; Bah, M.; Rivero-Cruz, J. F.; Lotina-Hennsen,
489 B. Mexican propolis flavonoids affect photosynthesis and seedling growth. *J.*
490 *Photochem. Photobiol. B Biol.* **2015**, *151*, 213–220.
491 (20) Dayan, F. E. Factors modulating the levels of the allelochemical sorgoleone in
492 *Sorghum bicolor*. *Planta* **2006**, *224*, 339–346.

493 (21) Rimando, A. M.; Dayan, F. E.; Czarnota, M. A.; Weston, L. A.; Duke, S. O. A new
494 photosystem II electron transfer inhibitor from *Sorghum bicolor*. *J. Nat. Prod.* **1998**,
495 *61*, 927–930.
496 (22) Barbosa, L. C. A.; Ferreira, M. lucia; Demuner, A. J. Preparation and phytotoxicity
497 of sorgoleone analogues. *Quim. Nova* **2001**, *24*, 751–755.
498 (23) Lima, L. S.; Barbosa, L. C. A.; de Alvarenga, E. S.; Demuner, A. J.; da Silva, A. A.
499 Synthesis and phytotoxicity evaluation of substituted *para*-benzoquinones. *Aust. J.*
500 *Chem.* **2003**, *56*, 625–630.
501 (24) Schulz, D.; Beese, P.; Ohlendorf, B.; Erhard, A.; Zinecker, H.; Dorador, C.; Imhoff,
502 J. F. Abenquines A-D: aminoquinone derivatives produced by *Streptomyces* sp.
503 strain DB634. *J. Antibiot. (Tokyo).* **2011**, *64*, 763–768.
504 (25) Nain-Perez, A.; Barbosa, L. C. A.; Maltha, C. R. A.; Forlani, G. First total synthesis
505 and phytotoxic activity of *Streptomyces* sp. metabolites abenquines. *Tetrahedron*
506 *Lett.* **2016**, *57*, 1811–1814.
507 (26) Nain-Perez, A.; Barbosa, L. C. A.; Maltha, C. R. A.; Forlani, G. Natural abenquines
508 and their synthetic analogues exert algicidal activity against bloom-forming
509 cyanobacteria. *J. Nat. Prod.* **2017**, *80*, 813–818.
510 (27) Sanner F., M. Python: A programming language for software integration and
511 development. *J. Mol. Graph.* **1999**, *17*, 57–61.
512 (28) Forli, S.; Huey, R.; Pique, M. E.; Sanner, M. F.; Goodsell, D. S.; Olson, A. J.
513 Computational protein–ligand docking and virtual drug screening with the
514 AutoDock suite Stefano. *Nat. Protoc.* **2016**, *11*, 905–919.
515 (29) Witt, H. T. Primary reactions of oxygenic photosynthesis. *Berichte der*
516 *Bunsengesellschaft für Phys. Chemie* **1996**, *100*, 1923–1942.
517 (30) Lotina-Hennsen, B.; Achnine, L.; Ruvalcaba, N. M.; Ortiz, A.; Hernández, J.;
518 Farfán, N.; Aguilar-Martínez, M. 2,5-Diamino-*p*-benzoquinone derivatives as
519 photosystem I electron acceptors: synthesis and electrochemical and
520 physicochemical properties. *J. Agric. Food Chem.* **1998**, *46*, 724–730.
521 (31) Nain-Perez, A.; Barbosa, L. C. A.; Picanço, M. C.; Giberti, S.; Forlani, G. Amino-
522 substituted *para*-benzoquinones as potential herbicides. *Chem. Biodivers.* **2016**, *13*,
523 1008–1017.
524 (32) Pereira, A.; Barbosa, L. C. A.; Demuner, A. J.; Silva, A. A.; Bertazzini, M.; Forlani,
525 G. Rubrolides as model for the development of new lactones and their aza analogs
526 as potential photosynthesis inhibitors. *Chem. Biodivers.* **2015**, *12*, 987–1006.

527 (33) Barbosa, L. C. A. *Espectroscopia no Infravermelho na caraterização de compostos*
528 *orgânicos*; Editora UFV, **2011**.
529 (34) Barbosa, L. C. A.; Demuner, A. J.; Alvarenga, E. S.; Oliveira, A.; King-Diaz, B.;
530 Lotina-Hennsen, B. Phytogrowth- and photosynthesis-inhibiting properties of
531 nostoclide analogues. *Pest Manag. Sci.* **2006**, *62*, 214–222.
532 (35) Barr, R.; Crane, F. L. Selective thiol inhibition of ferricyanide reduction in
533 photosystem II of spinach chloroplasts. *Biochem. Biophys. Res. Commun.* **1981**, *67*,
534 1190–1194.
535 (36) Lambreva, M. D.; Russo, D.; Polticelli, F.; Scognamiglio, V.; Antonacci, A.;
536 Zobnina, V.; Campi, G.; Rea, G. Structure/function/dynamics of photosystem II
537 plastoquinone binding sites. *Curr. Protein Pept. Sci.* **2014**, *15*, 285–295.
538 (37) Xiong, J.; Subramaniam, S.; Govindjee. Modeling of the D1/D2 proteins and
539 cofactors of the photosystem II reaction center: Implications for herbicide and
540 bicarbonate binding. *Protein Sci.* **1996**, *5*, 2054–2073.
541 (38) Rea, G.; Polticelli, F.; Antonacci, A.; Lambreva, M.; Pastorelli, S.; Scognamiglio,
542 V.; Zobnina, V.; Giardi, M. T. Computational biology, protein engineering, and
543 biosensor technology: a close cooperation for herbicides monitoring. In *Herbicides,*
544 *Theory and Applications*; Larramendy, M., Ed.; InTech, **2011**.
545 (39) Funar-Timofei, S.; Borota, A.; Crisan, L. Combined molecular docking and QSAR
546 study of fused heterocyclic herbicide inhibitors of D1 protein in photosystem II of
547 plants. *Mol. Divers.* **2017**, *21*, 437–454.
548 (40) Broser, M.; Glöckner, C.; Gabdulkhakov, A.; Guskov, A.; Buchta, J.; Kern, J.; Müh,
549 F.; Dau, H.; Saenger, W.; Zouni, A. Structural basis of cyanobacterial photosystem
550 II inhibition by the herbicide terbutryn. *J. Biol. Chem.* **2011**, *286*, 15964–15972.
551 (41) Singh, D. V.; Agarwal, S.; Kesharwani, R. K.; Misra, K. Molecular modeling and
552 computational simulation of the photosystem-II reaction center to address
553 isoproturon resistance in *Phalaris minor*. *J. Mol. Model.* **2012**, *18*, 3903–3913.
554 (42) Czarnota, M. A.; Paul, R. N.; Daynan, F. E.; Nimbal, C. I.; Weston, L. A. Mode of
555 action, localization of production, chemical nature, and activity of sorgoleone: a
556 potent PSII inhibitor in *Sorghum* spp. root exudates. *Weed Technology*, **2001**, *15*,
557 813-825.
558
559

560 **CAPTIONS TO FIGURES**

561

562 **Figure 1.** The structure of natural abenquines A-D, **1-4**, respectively, and some previously
563 synthesized analogues (**5-8**). The micromolar concentrations of these compounds that
564 inhibited by 50% the growth of the cyanobacterial strain *Synechococcus elongatus* PCC
565 6301 are also reported in parenthesis.[26]

566

567 **Figure 2**. Preparation of abenquine analogues **9-22**.

568

569 **Figure 3.** Effects increasing concentrations of compounds **10**, **14**, **15**, **21** on ferricyanide
570 reduction under basal, uncoupling or phosphorylating conditions.

571

572 **Figure 4.** Comparison of the effects of compounds **10**, **14**, **15**, **21** on the whole
573 chloroplastic electron transport chain and on a partial electron flow involving photosystem
574 II only.

575

576 **Figure 5.** Binding models of abenquine analogues **14** and **15** with the pocket site of PSII
577 from *Spinacia oleracea* (PDB ID: 3JCU).

578

Table 1. Natural Abenquines (**1-4**) and Analogues (**5-8**) as Inhibitor of the Light-Dependent Ferricyanide Reduction in Spinach Chloroplasts.

Compound	**IC_{50} (μM)**	**Compound**	**IC_{50} (μM)**
1 Abenquine A	279 ± 81	**5**	1.1 ± 0.1
2 Abenquine B	1487 ± 987	**6**	540 ± 258
3 Abenquine C	n.a.	**7**	56.9 ± 3.1
4 Abenquine D	n.a.	**8**	26.0 ± 1.9

n.a.- not active in the range tested (0.1 – 100 μM).

Table 2. Abenquine Analogues (**9-22**) Able to Inhibit the Light-Dependent Ferricyanide Reduction in Spinach Chloroplasts.

Compound	IC_{50} (μM)	Compound	IC_{50} (μM)
9	13 ± 2	**17**	0.38 ± 0.02
10	0.33 ± 0.02	**18**	2.6 ± 0.4
11	0.37 ± 0.02	**19**	43 ± 14
12	45 ± 6	**20**	n.a.[a]
13	4.7 ± 0.5	**21**	0.27 ± 0.01
14	0.18 ± 0.01	**22**	0.95 ± 0.48
15	0.19 ± 0.02	**23**[b]	n.a.[c]
16	3.6 ± 0.5		

[a] n.a. - not active in the range tested (0.01 – 100 μM).
[b] Analogue to **5** having a benzoyl instead of acetyl group.[26]
[c] 24% inhibition at 100 μM.

Figure 1

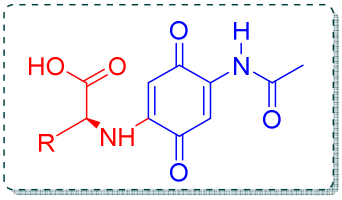

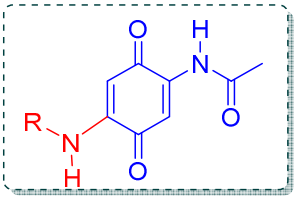

1 R = benzyl (9.6)
2 R = *sec*-butyl (13.8)
3 R = isopropyl (>100)
4 R = 3-methyl-1*H*-indol-3-yl (11.7)

5 R = benzyl (9.6)
6 R = 2-(pyrrolidin-1-yl)ethyl (0.8)
7 R = 2-(piperidin-1-yl)ethyl (0.6)
8 R = 2-(pyridin-2-yl)ethyl (3.8)

Figure 2

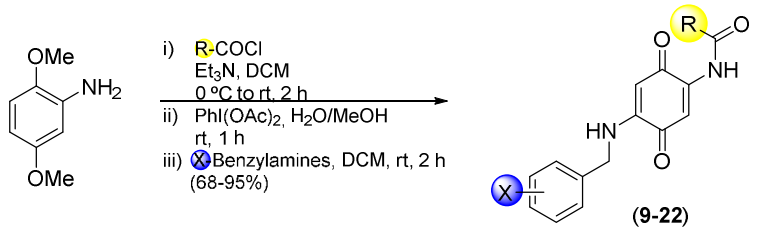

Compound	R	X			Analogue (%)
		orto	*meta*	*para*	
9	CH_3	F	H	H	90
10	CH_3	H	H	Cl	72
11	CH_3	H	Cl	H	68
12	CH_3	H	H	NO_2	76
13	CH_3	Br	H	H	85
14	CH_3	H	Br	H	92
15	CH_3	H	H	Br	78
16	CH_3	CH_3	H	H	70
17	CH_3	H	CH_3	H	68
18		H	H	H	90
19		H	H	H	82
20		H	H	H	95
21		H	H	H	75
22	O	H	H	H	86

Figure 3

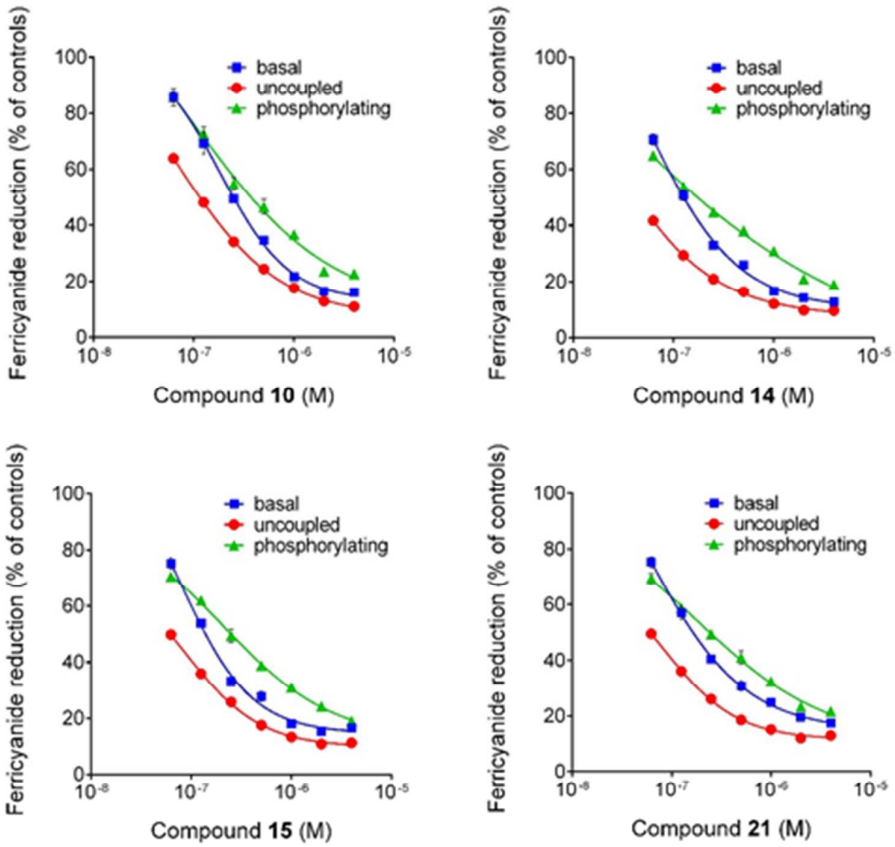
Ferricyanide reduction (% of controls)
basal
uncoupled
phosphorylating
Compound 10 (M)
Compound 14 (M)
Compound 15 (M)
Compound 21 (M)

Figure 4

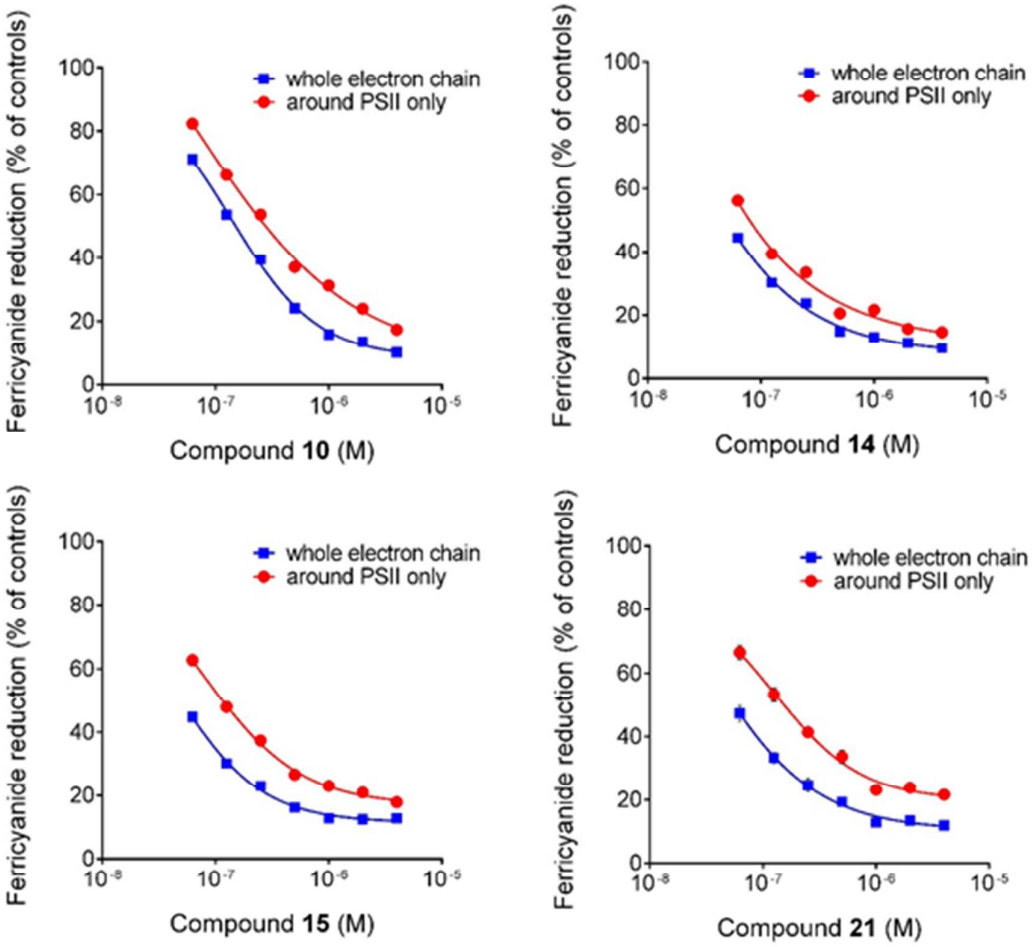

Figure 5

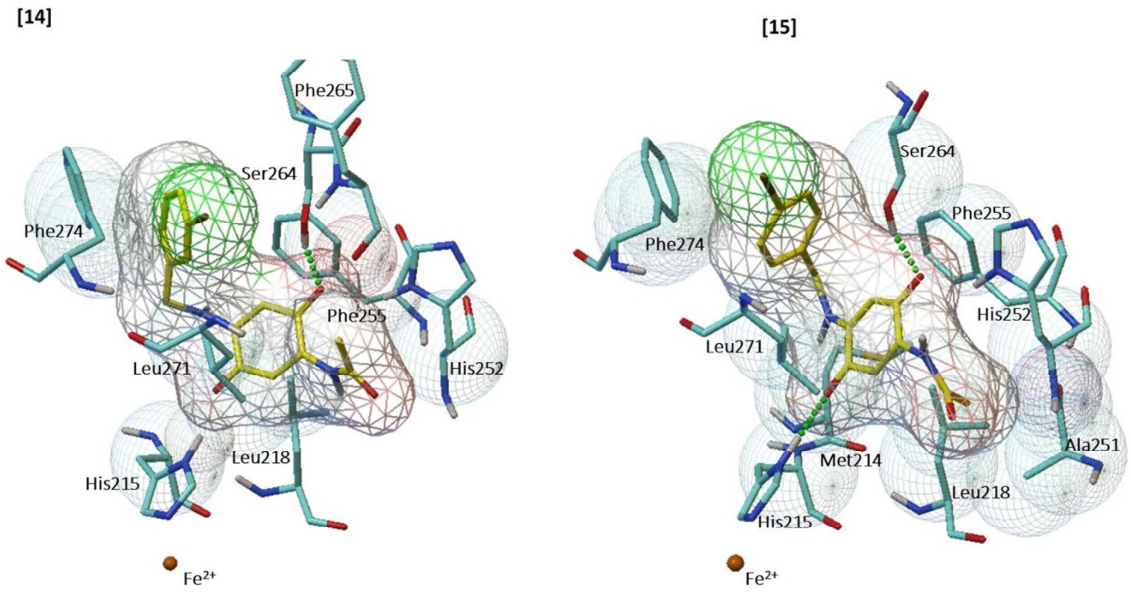
[14]
Phe265
Ser264
Phe274
Phe255
Leu271
His252
Leu218
His215
Fe2+
[15]
Ser264
Phe255
Phe274
His252
Leu271
Ala251
Met214
Leu218
His215
Fe2+

TABLE OF CONTENTS GRAPHIC

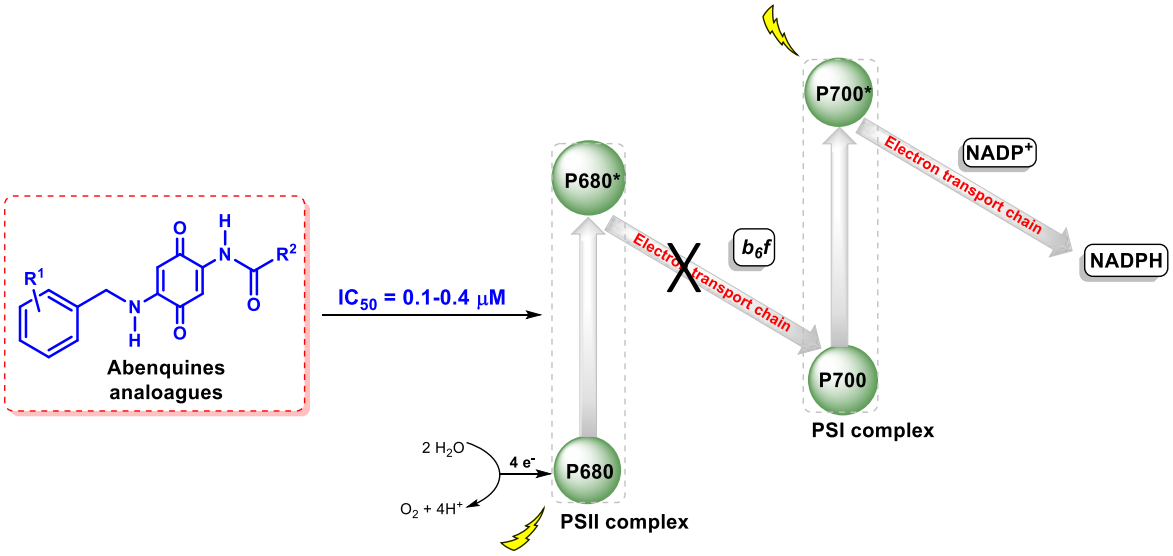

Abenquine analogues are potent inhibitors of photosynthetic electron transport chain.